DEPLOYMENT MECHANISM FOR A L-BAND HELIX ANTENNA IN 1-UNIT CUBESAT

Lara Fernandez[a,b,c,*], Marco Sobrino[a], Oriol Milian[a], Andrea Aguilella[a], Arnau Solanellas[a], Marc Badia[a], Joan Francesc Munoz-Martin[a,c], Joan Adria Ruiz-de-Azua[a,b,c], Miquel Sureda[c,d], Adriano Camps[a,c]

[a] *"CommSensLab" - UPC Unidad Maria de Maeztu, Dept. of Signal Theory and Communications, Universitat Politècnica de Catalunya BarcelonaTech*
[b] *Department of Network Engineering - UPC BarcelonaTech*
[c] *Institute of Space Studies of Catalonia (IEEC) - Space Science and Technology Research Group, CTE/UPC*
[d] *Department of Physics - UPC BarcelonaTech*

Abstract

Recently, there is a renewed interest in Earth Observation (EO) of the cryosphere as a proxy of global warming, soil moisture for agriculture and desertification studies, and biomass for carbon storage. Global Navigation Satellite System - Reflectometry (GNSS-R) and L-band microwave Radiometry have been used to perform these measurements. However, it is expected that the combination of both can largely improve current observations.

[3]Cat-4 mission aims at addressing this technology challenge by integrating a combined GNSS-R and Microwave Radiometer payload into a 1-Unit CubeSat. One of the greatest challenges is the design of an antenna that respects the envelope and stowage requirements of 1-Unit CubeSat, being able to work in the different frequency bands: Global Positioning System (GPS) L1-band (1575 MHz), GPS L2-band (1227 MHz), and microwave radiometry at 1400-1427 MHz. After a trade-off analysis, a helix antenna was found to be the most suitable option. This antenna has 11 turns equally distributed with 68.1 mm of diameter. This design generates an antenna with 506 mm of axial length, providing the maximum radiation gain in the endfire direction. Additionally, a counterweight

*Corresponding author
Email address: lara.fernandez.c@upc.edu (Lara Fernandez)

is added at the tip of the antenna to enhance the directivity, and it is used as gravity gradient technique. The deployment of this antenna in vacuum and extreme temperature conditions is the greatest mechanical challenge that needs to be addressed for the success of the mission.

This work presents a mechanical solution that enables to deploy the helix antenna from 25.5 mm (stowed configuration) to the final 506 mm (deployed configuration). By sequentially deploying different parts of the antenna, the final configuration is reached without impacting the attitude pointing of the CubeSat. This is accomplished using dyneema lines that are melted sequentially by commands. In addition, the deployment velocity, acceleration, and waving are presented as part of its characterization. The current test results in a Thermal Vacuum Chamber indicate also that the deployment can be achieved in -35 °C. The ^{3}Cat-4 CubeSat, with the L-band helix antenna, will be launched in Q4 2020 as part of the "Fly Your Satellite!" program of the European Space Agency (ESA).

Keywords: CubeSat, Nanosatellite, Helix, Deployable, Antenna

1. Introduction

There is an increasing interest in Earth Observation, specially in monitoring the Arctic region. This region is warming at twice the global rate, causing an extreme reduction of sea ice [1]. There are, different monitoring techniques to conduct useful measurements over polar regions. Recent studies have shown the possibility to obtain soil moisture [2], ocean wind speed [3], detect flooded regions or ice cover [4] with GNSS-Reflectometry (GNSS-R). Moreover, combining GNSS-R and Microwave L-Band Radiometry measures improves the resolution of soil moisture and ocean salinity data products [5].

The ^{3}Cat-4 mission [6] aims at demonstrating the capabilities of a 1 Unit (1U) CubeSat to perform dual-band (L1 and L2) GNSS-R and Microwave Radiometry. The payload is composed by the Flexible

Microwave Payload 1 (FMPL-1) [7], the Nadir Antenna and Deployment Subsystem (NADS), which is the downlooking antenna, and an uplooking active antenna.

To fulfill the mission goals the NADS antenna has to be directive (i.e. more than 12 dB of directivity), left hand circularly polarized, and it has to occupy less than 0.3U. A widely used solution for GNSS-R payloads is to use an array of patch antennas which are placed on an external face of the satellite, as it has been done in TechDemoSat-1 [8] and 3Cat-2 [9]. Patch antenna arrays with the required directivity are composed by 6 elements, needing a 6U face to allocate the antennas. So, although this solution is simple in terms of mechanical interfaces, it is not valid for the 3Cat-4 mission since it is a 1U CubeSat.

Another solution, are helical antennas. These antennas are initially stowed in the satellite to then be deployed in orbit. Some missions have flown with commercial helical antennas, such as GOMX-1 [10] and GOMX-3 [11] as payload antennas, for ADS-B data acquisition. Also, Lacuna Space [12] has launched an Internet of Things (IoT) payload with an helical antenna on-board a nanoavionics spacecraft. Moreover, there is a commercial solution for a quadrifilar helical antenna [13] but it occupies half a CubeSat Unit.

There are also some studies on deployable antennas, [14], [15], [16], [17], but most of them are focused on the radiofrequency design, and performance of the antenna rather than in the deployment mechanism itself, which is a critical part. Other solutions, such as reflector antennas, reflect arrays and membrane antennas are proposed by Authors in [18], but these solutions are not suitable for the 3Cat-4 mission due to the space restriction of 0.3U.

This article presents the design, functional and environmental results of the NADS. This subsystem includes an L-Band helix antenna with Left Hand Circular Polarization (LHCP) and the deployment mechanism for this antenna, in less than 0.3 CubeSat Units. The

arcticle is organized as follows, Section 2 describes the different mechanical parts of the NADS, and their functionalities. Section 3 presents the ambient tests, vibration tests and thermal vacuum tests results. Finally, section 4 presents the conclusions.

2. Antenna Deployment Mechanism

The NADS has two different configurations stowed, Figure 1, and deployed, Figure 2. The deployment mechanism has been designed to ensure safety and functionality during launch, i.e. no unexpected deployments or resonances below 100 Hz. Moreover, the design also ensures the correct deployment of the antenna, and the expected RF performance once it is deployed. Finally, the a gravity boom is added to help compensating the aerodynamic drag that the antenna produces.

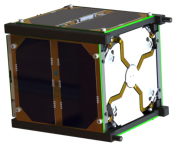

Figure 1: NADS in stowed configuration

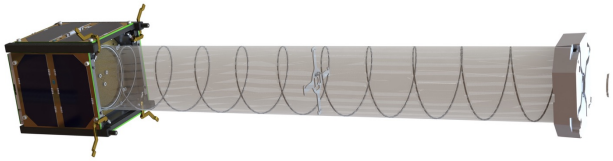

Figure 2: NADS in deployed configuration

2.1. Subsystem Description

The NADS has a total mass of 253 gr, the envelope of the Subsystem for both configurations can be seen in Figure 4 and the dimensions of the antenna are given in Table 1. The different parts that

conform the subsystem can be seen in Figure 3. and the materials can be seen in Table 2, some of the parts have surface treatments to prevent oxidation in space.

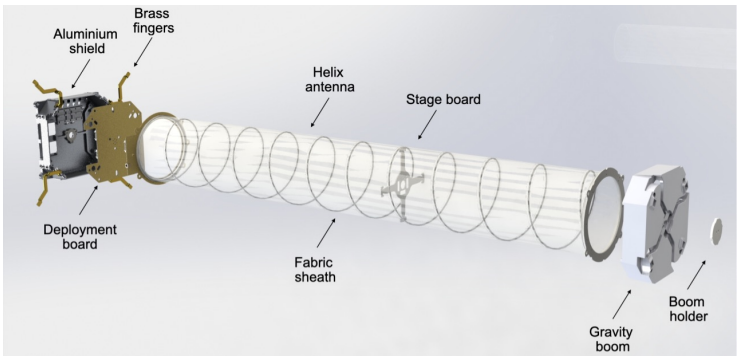

Figure 3: NADS exploded view

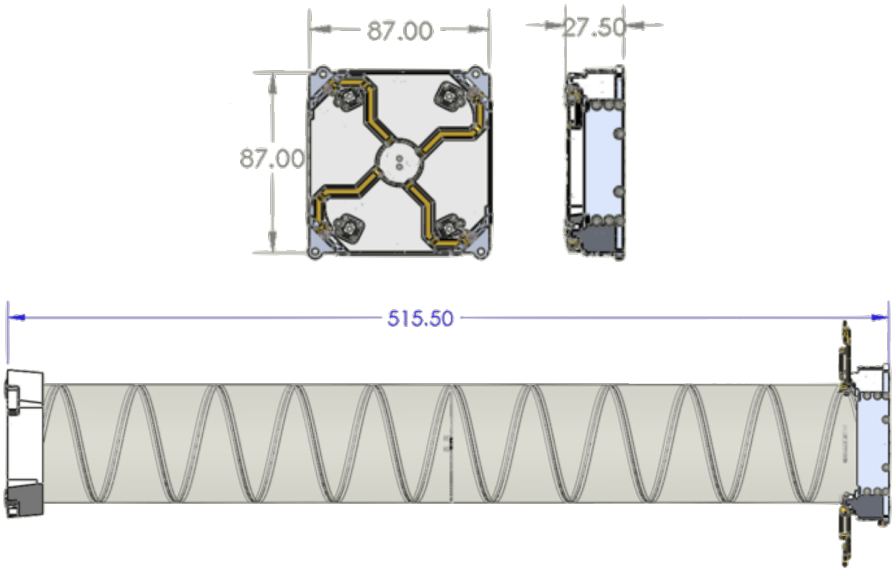

Figure 4: Dimensions of the Subsystem

In stowed configuration the NADS is held by five melting lines. One melting line holds half of the antenna, this line is secured in the Stage Board. Two more melting lines hold the gravity boom keeping the whole antenna stowed. Finally,

N	Number of turns	11
d	Diameter of the antenna (mm)	68
ϕ	Section of the coil (mm)	1
S	Spacing between turns (mm)	46
α	Angle of incidence (^{o})	12.36
A	Deployed axial length (mm)	506
a	Stowed axial length (mm)	11

Table 1: Dimensions of the antenna

Part	Material	Surface Treatment
Aluminum Shield	Aluminium 7075	SurTec Alodine
Brass fingers	Brass	-
Deployment board	FR-4	-
Helix Antenna	Spring steel	Tin
Fabric sheath	PTFE fabric	-
Stage board	FR-4	-
Gravity boom	PTFE	-
Boom holder	PTFE	-

Table 2: Materials of NADS parts

the four brass fingers prevent the antenna and gravity boom from moving, these fingers are secured by the boom holder. The boom holder is also held by two melting lines. Both the gravity boom and boom holder have redundant melting lines to prevent an unexpected deployment in case of failure on one of the lines.

The melting lines are arranged in the Aluminium shield so that there is contact between the lines and the burning resistors placed in the deployment board. There are primary resistors and redundant resistors.

2.2. Deployment Sequence

The deployment is performed in three stages. The first stage releases the boom holder and the fingers, the second releases the gravity boom deploying half of the antenna, and the finals step deploys the complete antenna by releasing the stage PCB.

The deployment board includes feedback switches. The switches indicate if the melting lines are burnt, i.e. stage deployed, or not. If the deployment switches were to fail, the deployment of the antenna can be verified by executing the payload over a calibration area and comparing the power received with the expected value. Additionally, a replica of the NADS the Qualification Model will be in the FlatSat, so if any error were to occurred the issue can be replicated and analized.

The deployment is executed through telecommand (TC). There is one TC for each melting line and the deployment sequence only proceeds to the next stage if the previous one has positive feedback from the switches. Moreover, in between the deployment of the different stages it is necessary to wait until the attitude of the satellite is stabilized, from an operator point of view. During the deployment of the NADS, the satellite is in Nadir Pointing mode, so pointing towards the surface of the Earth.

Once the antenna is deployed the fabric sheath maintains the shape of the helix.

3. Verification Campaigns

In order to verify the design of the deployment mechanism a qualification model of the subsystem has been tested in ambient conditions by performing antenna deployments. Moreover, it has also been tested in the environmental conditions that will be experienced during launch including vibration tests, and in orbit with thermal vacuum tests.

3.1. Ambient tests

The verification of the antenna design has been conducted by performing ten consecutive successful deployment tests in ambient conditions.

To perform these tests the antenna is placed on a test bench, which holds the aluminium shield of the antenna as well as the gravity boom. This configuration allows to deploy the antenna in a horizontal position, minimizing the effect of gravity by attaching the gravity boom (i.e. the main moving part in the deployment) to a bearing that allows the antenna to move in the axial direction.

Figure 5 shows the deployment performed in one of the ambient tests and Figure 5d has a QR code that redirects to the deployment video of the antenna.

3.2. Vibration tests

The goal of vibration testing is to ensure that the first resonance of the subsystem is above 100 Hz and that the subsystem is able to withstand the structural stress suffered during launch by being functional after.

The subsystem has undergone a sine sweep test, which emulates the acceleration of the launcher. As well as, a random vibration test, emulating the structural stress induced by the rocket. Before and after each of the tests a resonance survey is performed to verify that the subsystem has not suffered any mechanical damage. The profiles used for the tests were obtained from a launcher and can be seen in Tables 3, 4 and 5, in the case of the random vibration the load was 11.92 grms.

Frequency (Hz)	Value (g)
20 - 2000	0.4

Table 3: Resonance survey test profile

The NADS has been vibrated in all three axes and the metrics have been obtained using monoaxial accelerometers. Three different

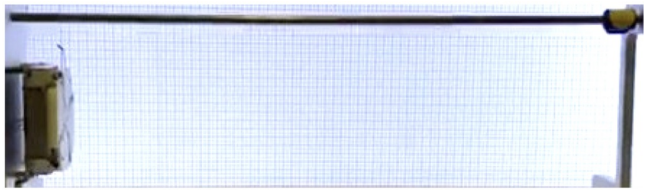

(a) Subsystem in stowed configuration

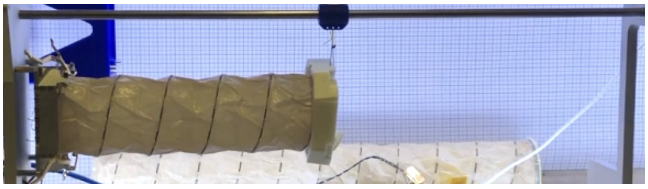

(b) First and second stages deployed

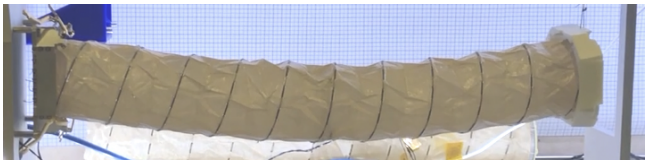

(c) Subsystem in deployed configuration

(d) Deployment video

Figure 5: NADS ambient deployment test sequence

accelerometers are placed for the test and the setup for the tests is shown in Figure 6. The green accelerometer has a dynamic range of 50 g and the red one can measure up to 500 g. The green accelerometer is placed to obtain accurate readings of the resonance surveys and the rest of the tests. The red one, having a higher dynamic range is placed to measure if there are amplifications over 50 g for the since and random tests, although the resolution is not valid to have

Frequency (Hz)	Value (g)
5.0	1.25
10.0	4.00
20.0	4.00
70.0	2.25
110.0	450.00
125.0	450.00

Table 4: Sine sweep test profile

Frequency (Hz)	Value (g^2/Hz)
20	0.228
153	0.0228
190	0.396
250	0.396
750	0.220
2000	0.072

Table 5: Random vibration test profile

accurate measures in the resonance survey. Moreover, a third 50 g accelerometer is placed in the slip plate to be the control reference for the Shaker.

The resonances of the subsystem after sine sweep and random vibrations can be seen in Figures 7, 8 and 9. The measurements are taken with three different accelerometers. One is the control (blue), which adjusts the stress put to the subsystem. The other two are measurements of the subsystem. The resonant frequencies can be found in Table 6.

The success criteria of the test campaign is based on a comparison between the first resonance survey and the last one. If the resonances of the subsystem have changed, that implies a mechanical change in

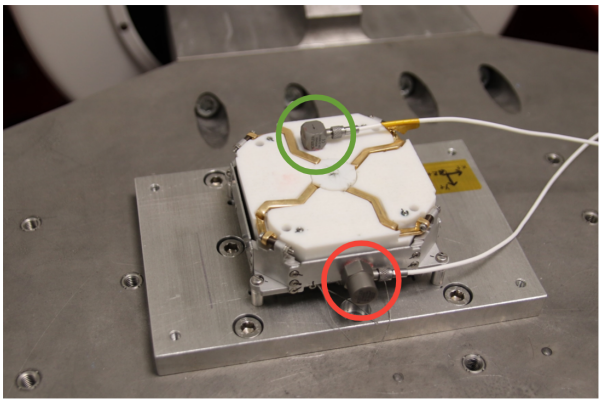

Figure 6: NADS assembled in the Shaker slip table

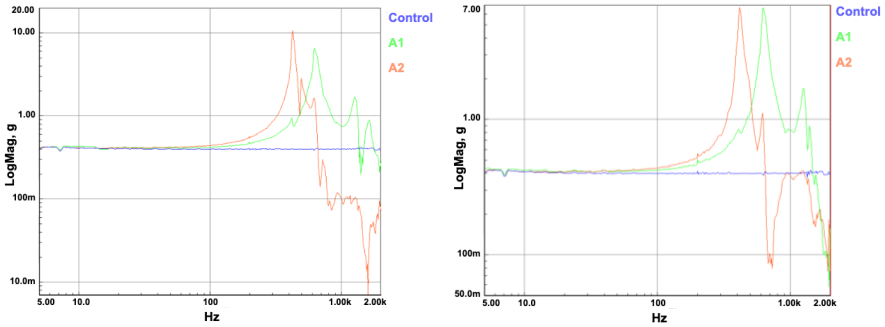

(a) Initial resonance survey

(b) Final resonance survey

Figure 7: Resonance surveys on X axis

	X	Y	Z
Resonant frequency (Hz)	600	700	500

Table 6: First resonant frequencies

the Subsystem. Comparing the results from the tests, the spectra measured by accelerometer 1 (green) there are no major differences in the natural frequencies. The measurements from accelerometer 2 (red) are not valid for this test, since the resolution of the accelerometer is not accurate enough to measure the low excitation of a resonance survey test.

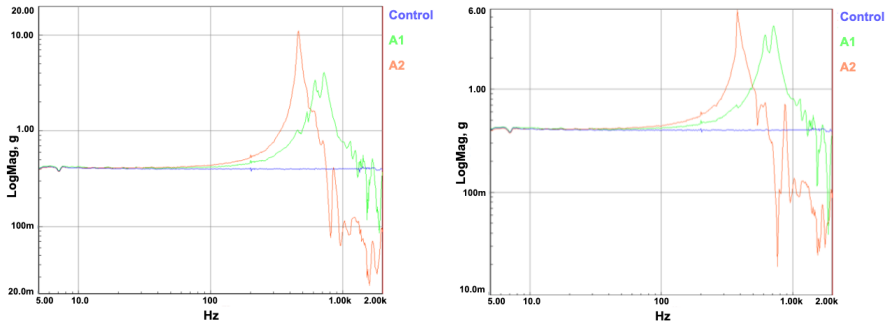

(a) Initial resonance survey (b) Final resonance survey

Figure 8: Resonance surveys on Y axis

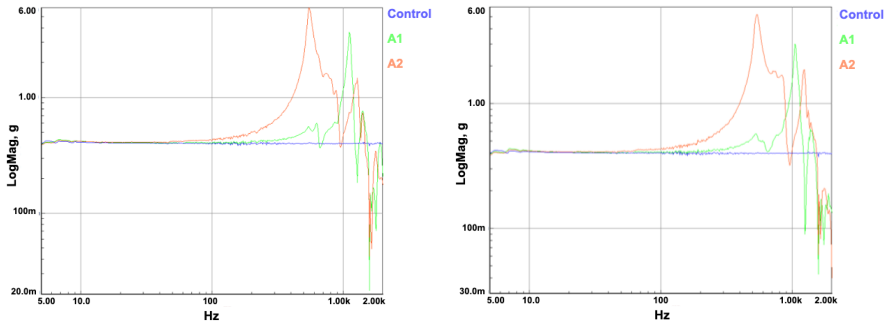

(a) Initial resonance survey (b) Final resonance survey

Figure 9: Resonance surveys on Z axis

Moreover, a visual inspection on the fasteners and visible parts of the subsystem are also done, as it can be seen in Figure 10, the subsystem showed no movement in parts or fasteners after the vibration tests.

Finally, a deployment test was done with the same setup used for the Ambient Tests. The objective of this test was not only to verify the deployment functionality, but also to ensure that no movement in the melting lines has occurred during vibrations. The outcome of this test was positive, achieving a full deployment of the antenna. For all the above results, the test campaign has been considered successful.

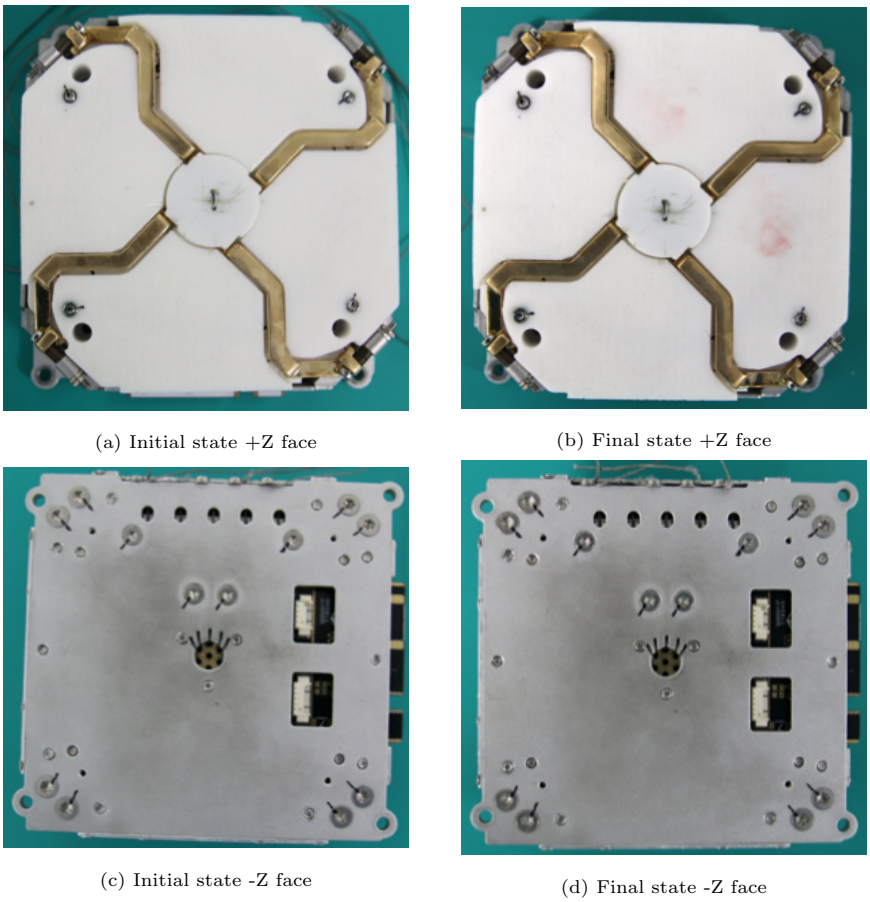

(a) Initial state +Z face

(b) Final state +Z face

(c) Initial state -Z face

(d) Final state -Z face

Figure 10: Visual inspection of the Subsystem

3.3. Thermal Vacuum Tests

The goal of the Thermal Vacuum Tests is to verify that the NADS is capable of deploying in vacuum and extreme temperatures conditions. This emulates the environment that the subsystem will face when it is in orbit.

The deployment test was only performed in cold conditions. These conditions are the most critical for the mechanical parts, since some parts could stiffen at cold temperatures, preventing the deployment. The operational temperature of the Subsystem are between 80 °C and -40 °C. Thus, considering that the test is performed at Qualification

Level, the temperature for the deployment is -35 °C.

The thermal profile used in the test can be seen in Figure 11. The temperature ramp is set to 2 °C/ minute, with a dwell time of 1 hour and a plateau of an additional hour to execute the deployment.

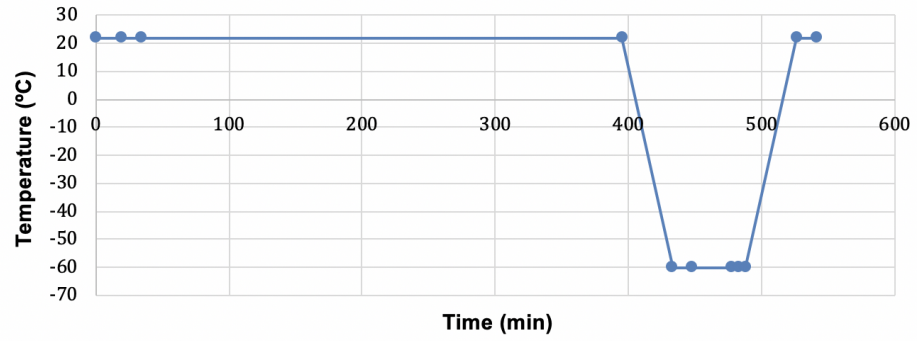

Figure 11: Thermal profile

The setup for the test was the same as for the ambient tests, using the test bench. So, the NADS was placed in the test bench inside a Thermal Vacuum Chamber (TVAC).

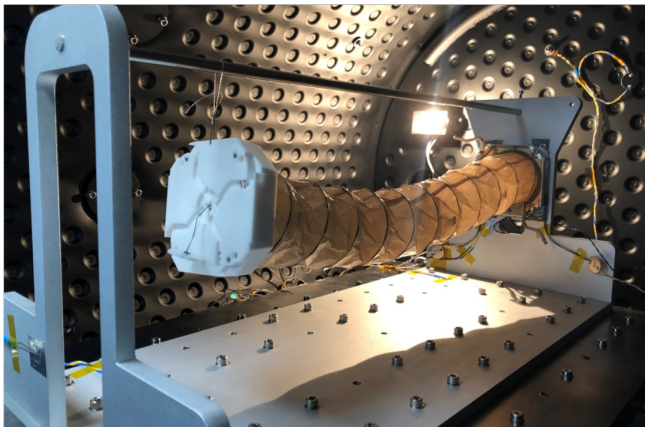

Figure 12: NADS deployed inside ESEC-Galaxia TVAC `https://www.esa.int/Education/CubeSats_-_Fly_Your_Satellite/CubeSat_Support_Facility`

The test was considered successful since the antenna was fully deployed in vacuum conditions and at -35 °C. Moreover, the electronics also worked in

vacuum and cold conditions.

4. Conclusions

This article summarizes the design and characterisation tests of a deployment mechanism for an helical antenna, following the CubeSat standard. This mechanism will fly on the ^{3}Cat-4 satellite, it conforms the Nadir Antenna and Deployment Subsystem (NADS).

The NADS has two different configurations, it is stowed during launch and deployed when the satellite is in orbit. The design has considered safety, functional and performance requirements to ensure success on both configurations and also on the deployment of the antenna.

The subsystem has been verified through ambient testing, performing deployments of the antenna in order to verify the design. It has also been vibrated, to ensure the correct functionality during launch and the capability to deploy once it is orbiting. Finally, the correct deployment of the antenna in space conditions has been verified through a thermal vacuum test at -35 ^{o}C.

References

[1] G. C. Smith, et al., Polar Ocean Observations: A Critical Gap in the Observing System and Its Effect on Environmental Predictions From Hours to a Season, Frontiers in Marine Science 6 (2019) 429. doi:10.3389/fmars.2019.00429.
URL https://www.frontiersin.org/article/10.3389/fmars.2019.00429

[2] A. Camps, H. Park, M. Pablos, G. Foti, C. Gommenginger, P.-W. Liu, J. Judge, Sensitivity of GNSS-R Spaceborne Observations to Soil Moisture and Vegetation, IEEE Journal of Selected Topics in Applied Earth Observations and Remote Sensing 9 (2016) 1–13. doi:10.1109/JSTARS.2016.2588467.

[3] M. Clarizia, C. Ruf, Wind Speed Retrieval Algorithm for the Cyclone Global Navigation Satellite System (CYGNSS) Mission, IEEE Transactions on Geoscience and Remote Sensing (2016) 1–14doi:10.1109/TGRS.2016.2541343.

[4] A. Alonso-Arroyo, V. U. Zavorotny, A. Camps, Sea ice detection using u.k. tds-1 gnss-r data, IEEE Transactions on Geoscience and Remote Sensing 55 (9) (2017) 4989–5001. doi:10.1109/TGRS.2017.2699122.

[5] E. Valencia, A. Camps, N. Rodriguez-Alvarez, I. Ramos-Perez, X. Bosch-Lluis, H. Park, Improving the accuracy of sea surface salinity retrieval using GNSS-R data to correct the sea state effect, Radio Science 46 (06) (2011) 1–11. doi:10.1029/2011RS004688.

[6] J. A. Ruiz-de-Azua, J. F. Muñoz, L. Fernández, M. Badia, D. Llavería, C. Diez, A. Aguilella, A. Pérez, O. Milian, M. Sobrino, A. Navarro, H. Lleó, M. Sureda, M. Soria, A. Calveras, A. Camps, 3cat-4 mission: A 1-unit cubesat for earth observation with a l-band radiometer and a gnss-reflectometer using software defined radio, in: IGARSS 2019 - 2019 IEEE International Geoscience and Remote Sensing Symposium, 2019, pp. 8867–8870. doi:10.1109/IGARSS.2019.8898317.

[7] J.F. Munoz-Martin, N. Miguelez, R. Castella, L. Fernandez, A. Solanellas, P. Via, and A. Camps, 3Cat-4: Combined GNSS-R, L-Band Radiometer with RFI Mitigation, and AIS Receiver for a I-Unit Cubesat Based on Software Defined Radio, 2018 IEEE International Geoscience and Remote Sensing Symposium (IGARSS) (2018) 1063–1066doi:10.1109/IGARSS.2018.8519037.

[8] ESA, Techdemosat-1 (technology demonstration satellite-1) / tds-1, accessed: March 2020 (2010).
URL https://earth.esa.int/web/eoportal/satellite-missions/t/techdemosat-1

[9] H. Carreno-Luengo, A. Camps, P. Via, J. F. Munoz, A. Cortiella, D. Vidal, J. Jané, N. Catarino, M. Hagenfeldt, P. Palomo, S. Cornara, 3cat-2—an experimental nanosatellite for gnss-r earth observation: Mission concept and analysis, IEEE Journal of Selected Topics in Applied Earth Observations and Remote Sensing 9 (10) (2016) 4540–4551. doi:10.1109/JSTARS.2016.2574717.

[10] L. Alminde, K. Kaas, M. Bisgaard, J. Christiansen, D. Gerhardt, Gomx-1 flight experience and air traffic monitoring results, in: AIAA Small Satellites Conference, AIAA, 2014.

[11] D. Gerhardt, M. Bisgaard, L. Alminde, R. Walker, M. A. Fernandez, A. Latiri, J.-L. Issler, Gomx-3: Mission results from the inaugural esa in-orbit demonstration cubesat, in: AIAA Small Satellites Conference, AIAA, 2016.

[12] L. Space, Lacuna, accessed: March 2020 (2019).
URL https://www.lacuna.space/

[13] H. C. Technologies, Helios deployable antenna, (Accessed: March 2020).
URL https://www.helicomtech.com/helios-deployable-antenna

[14] M. Sakovsky, S. Pellegrino, J. Costantine, Rapid Design of Deployable Antennas for CubeSats: A tool to help designers compare and select antenna topologies, IEEE Antennas and Propagation Magazine 59 (2) (2017) 50–58. doi:10.1109/MAP.2017.2655531.

[15] J. Costantine, Y. Tawk, I. Maqueda, M. Sakovsky, G. Olson, S. Pellegrino, C. Christodoulou, UHF Deployable Helical Antennas for CubeSats, IEEE Transactions on Antennas and Propagation 64 (2016) 1–1. doi:10.1109/TAP.2016.2583058.

[16] A. Takacs, H. Aubert, D. Belot, H. Diez, Miniaturization of Compact Quadrifilar Helix Antennas for Telemetry, Tracking and Command Ap-

plications, Progress In Electromagnetics Research C 60. doi:10.2528/PIERC15072606.

[17] G. Knott, C. Wu, A. Viquerat, Deployable bistable composite helical antennas for small satellite applications, 2019. doi:10.2514/6.2019-1260.

[18] Y. Rahmat-Samii, V. Manohar, J. M. Kovitz, For satellites, think small, dream big: A review of recent antenna developments for cubesats., IEEE Antennas and Propagation Magazine 59 (2) (2017) 22–30. doi:10.1109/MAP.2017.2655582.